J. Fluid Mech. (1973), *vol.* 61, *part* 3, *pp.* 583–607
Printed in Great Britain

Topographic Rossby waves in a rough-bottomed ocean

By PETER RHINES
Woods Hole Oceanographic Institution, Massachusetts
AND FRANCIS BRETHERTON
Department of Earth and Planetary Sciences, The Johns Hopkins University

(Received 21 May 1973)

The object is to predict the nature of small-amplitude long-period oscillations of a homogeneous rotating fluid over a 'sea bed' that is nowhere level. Analytically, we are limited to special choices of bottom topography, such as sinusoidal corrugations or an undulating continental slope, so long as the topographic restoring effect equals or exceeds that due to planetary curvature (the beta-effect). (Very slight topographic features, on the other hand, provide weak, resonant interactions between Rossby waves.)

Integral properties of the equations, and computer experiments reported elsewhere, verify the following results found in the analytical models: typical frequencies of oscillation are $\lesssim f\delta$, where f is the Coriolis frequency and δ measures the fractional height of the bottom bumps; an initially imposed flow pattern of large scale will rapidly shrink in scale over severe roughness (even the simplest analytical model shows this rapid change in spatial structure with time); and energy propagation can be severely reduced by roughness of the medium, the energy velocity being of order $f\delta a$, where a is the horizontal topographic scale (although in an exceptional case, the sinusoidal bottom, the group velocity remains finite for vanishingly small values of a).

1. Introduction

The complex shape of the ocean bottom and coastal boundaries affects currents and waves in many ways, as the diversity of recent literature on the subject indicates. Swallow's discovery of vigorous eddies in the western North Atlantic stimulated interest especially in transient motions, for the mean circulation appears to be the weaker in the deep sea. The related 'bumpy spin-up' problem bears on other geo- and astrophysical situations (Hide, private communication).

This paper deals with a linearized model of slow oscillations in a homogeneous fluid. They are a generalized version of Rossby waves satisfying an equation for the local conservation of barotropic potential vorticity. The depth h thus appears as a variable coefficient in the two-dimensional wave equation. In the beta-plane approximation, the earth's curvature provides a uniform restoring effect, which is distorted by complex topography. The problem is, at first sight, similar to classical situations involving membranes of non-uniform mass density or high-energy particles moving in a complex potential field.

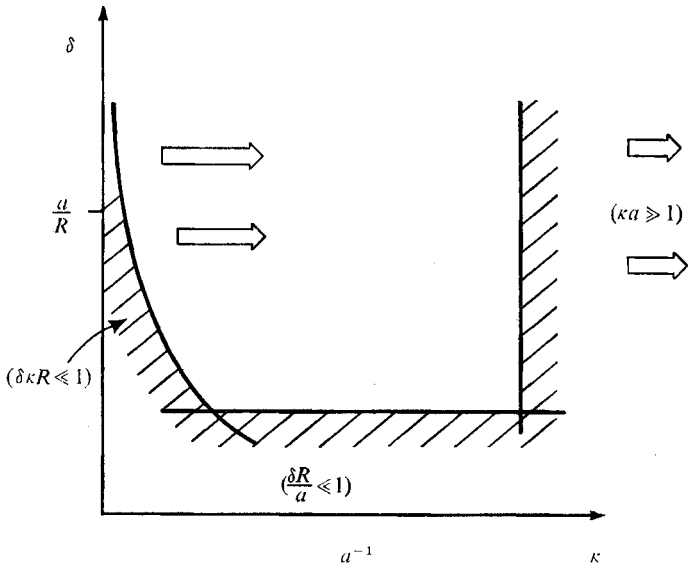

FIGURE 1. Location, with respect to δ and k, of various theories of waves in non-uniform media; δ is the typical, fractional change in depth, k the initially imposed wavenumber, and a the dominant topographic scale. As time progresses, solutions often tend to move to the right on the diagram (arrows).

Most theories for such problems, however, have rather severe limitations, even after restricting the dynamics to be linear. Success has depended on the inhomogeneities of the medium being *gradual*, *slight* or *abrupt*. The corresponding approaches may be called, respectively, ray theory, resonant interaction, or weak-scattering, theory, and Schrödinger, or strong-scattering, theory. In addition certain smoothly varying media yield exact wave solutions in non-trigonometric functions. What is missing from the list is some approach to the problem of a medium whose inhomogeneity is neither small nor localized nor gradual, for this seems to be the nature of much of the sea bed.

Figure 1 is a sketch of these various regions of δ, k space where the theories apply, δ being the typical topographic height divided by the mean ocean depth, and k the wavenumber characterizing the initially imposed flow field. If we suppose the bottom topography to be homogeneous in space and characterized by a dominant horizontal scale a, then geometrical optics (gradual variations; Smith 1971; Rhines 1971*a*) apply at the right-hand side, $ka \gg 1$. Weak scattering (slight variations relative to the beta-effect; Rhines 1970*b*) occurs where $\delta \ll \beta a/f$ ($\sim a/R_e$), β being df/d (latitude) and R_e the earth's radius. Weak scattering also applies with long waves in $\delta \ll (kR_e)^{-1}$ (Robinson & Stommel 1959). The theory of waves in random media (e.g. Frisch 1968) applies to this last regime, but topographic effects are probably too strong to be thus approached.

The interesting central region $ka \sim 1$, $\delta R_e/a \sim 1$ has been penetrated with solutions for isolated abrupt variations in the medium (Rhines 1969), but there appears to have been little discussion of the case, so relevant to the ocean, where the variations in the medium are everywhere significant. [Some computer experi-

ments have, however, been done for the related problem of vibrating molecular chains of mixed species (Dean 1967).] It is of particular interest to decide what characteristic periods and scales of waves then occur, and how efficiently they can transmit energy.

The plan of the paper is, first, to derive a solution for free waves over a sinusoidal bottom in § 2. There is no average restoring effect ($\beta = 0$), yet waves persist even at scales much greater than that of the bottom (this is a peculiar limit of Mathieu's equation).

A smooth restoring effect (β-effect or a broad bottom slope) is then included, and a slight extension made to the case with several Fourier components of depth (yet all oriented in the same direction). Scales $L \lesssim a$ for which the above solution fails (the very centre of figure 1) are considered, using known properties of Mathieu's equation. Roughly the same frequency, $\sim f\delta$, occurs but energy propagation is severely reduced. For $L \ll a$, the ray-theory limit, the channelling of waves along f/h contours becomes nearly total.

In § 3 a three-dimensional sea bed is allowed. The perturbation approach for slight depth variations is criticized. Simple solutions are found for the depth dependence $h = H\exp(e^{-x}\sin y)$, where (x, y) are horizontal co-ordinates. The tendency of three-dimensional topography to reduce the energy flux is discussed. Integral properties of the equations are invoked here to suggest that the predicted time and length scales are generally similar to those found above. A new approach to the 'very' rough problem is outlined, and some analogous behaviour from solid-state physics described. An appendix gives some general properties of the eigenvalue problem for a closed basin.

2. Two-dimensional topography

The linearized inviscid equation for waves of low frequency in a homogeneous β-plane ocean describes the changes in relative vorticity due to motion northward or up a slope:

$$\nabla.(h^{-1}\nabla\psi) - \frac{1}{i\sigma}\left(\nabla\psi \times \nabla\frac{f}{h}\right).\hat{\mathbf{i}} = 0. \tag{2.1}$$

Here, $\psi(\hat{x}, \hat{y})\, e^{-i\sigma t}$ is the total stream function for the mass flux, $O\hat{x}$ and $O\hat{y}$ Cartesian axes directed east and north respectively, t the time, h the depth of the fluid (ignoring for simplicity motion of the free surface), f the latitude-dependent Coriolis parameter and $\hat{\mathbf{i}}$ a vertical unit vector. The assumption of linearity requires $\epsilon/\delta \ll 1$, ϵ being the Rossby number U/fa, based on the horizontal scale of the topography a, typical velocity U and typical fractional height of the roughness δ. It is a severe restriction saying that the excursions of the particles must not carry them completely over the bumps of interest. Scales a so small that $\epsilon/\delta > 1$ are effectively smoothed by the nonlinearities, if they involve no net change in depth. The assumption of columnar motion implicit in (2.1) is more easily satisfied, essentially requiring $(\sigma H/fa)^2 \ll 1$ for an f-plane model. Frequently this means just that the bottom slope $\ll 1$. The neglect of stratification implies $NH/fa \ll 1$, where N is the mean buoyancy frequency.

Long waves over a sinusoidal bottom

We consider first the solutions when the depth $h(y)$ has straight contours and undulates in a continuous sine wave. For simplicity f is at first taken to be constant (no β-effect), so that in the absence of topography there would be no waves at all. The height of the undulations is kept small but this is a secondary matter. With

$$\ln h = 1 + \delta \sin(\hat{y}/a) + \ln H$$

and separating out a wavelike dependence on $\hat{x}$ and t, the equation is nearly Mathieu's equation:

$$\hat{\psi}_{yy} - \delta \cos y \hat{\psi}_y + [-k^2 + (\delta k/\omega)\cos y]\hat{\psi} = 0, \tag{2.2}$$

where

$$\psi = \hat{\psi}(y)\, e^{i(\hat{k}\hat{x} - \sigma t)}, \quad (x, y) = (\hat{x}/a, \hat{y}/a), \quad \omega = \sigma/f, \quad k = \hat{k}a.$$

The classical solutions describing the stabilization of an inverted pendulum by the oscillation of its support hint that, in the present problem, some sort of wavelike solutions will be found (and be well behaved in an unbounded medium) even when the restoring effect (the bottom slope) vanishes in the mean.

General considerations show that $\omega \lesssim \delta$, so that we adopt the scaling $\omega \sim \delta \sim k \ll 1$ appropriate to long waves. Then the topography is far more important in the vertical stretching (the last term) than in the second term.

A long-wave expansion may be made in powers of k, allowing $\hat{\psi}$ to depend separately on y and $Y \equiv ky$:

$$\hat{\psi} = \psi^{(0)}(y, Y) + k\psi^{(1)}(y, Y) + \ldots,$$

yielding

$$\left.\begin{aligned} &\psi^{(0)}_{yy} = 0 \quad \text{at} \quad O(1), \\ &\psi^{(1)}_{yy} + 2\psi^{(0)}_{yY} - \frac{\delta}{k}\cos y \left(\psi^{(0)}_y - \frac{k}{\omega}\psi^{(0)}\right) = 0 \quad \text{at} \quad O(k), \\ &\psi^{(2)}_{yy} + 2\psi^{(1)}_{yY} + \psi^{(0)}_{YY} - \frac{\delta}{k}\cos y \left(\psi^{(0)}_Y + \psi^{(1)}_y - \frac{k}{\omega}\psi^{(1)} - \psi^{(0)}\right) = 0 \quad \text{at} \quad O(k^2). \end{aligned}\right\} \tag{2.3}$$

Requiring each $\psi^{(n)}$ to be bounded as $y \to \infty$ with Y fixed, the first two orders yield

$$\psi^{(0)} = \psi^{(0)}(Y) \text{ only}, \quad \psi^{(1)} = (\delta/\omega)\cos y \psi^{(0)}.$$

The $O(k^2)$ equation is then

$$\psi^{(0)}_{YY} + \psi^{(0)}\left[-1 + \frac{1}{2}\frac{\delta^2}{\omega^2}\right] = -\psi^{(2)}_{yy} + \psi^{(0)}_Y\left[\frac{2\delta}{\omega}\sin y + \frac{\delta}{k}\cos y\right] - \psi^{(0)}\left[\frac{\delta^2}{2k\omega}\sin 2y + \frac{\delta^2}{2\omega^2}\cos 2y\right].$$

Now terms independent of y (the left-hand side) must sum to zero to prevent secular growth of $\psi^{(2)}$. This determines the gradual variation of $\psi^{(0)}$:

$$\psi^{(0)}_{YY} + \left|\tfrac{1}{2}(\delta/\omega)^2 - 1\right|\psi^{(0)} = 0,$$

so that there are solutions

$$\left.\begin{aligned} \psi^{(0)} &= e^{\pm i\lambda Y}, \\ \omega^2 &= \delta^2/2(\lambda^2+1) = \tfrac{1}{2}\delta^2\cos^2\theta, \end{aligned}\right\} \tag{2.4}$$

with θ defined as the angle between the propagation vector $\mathbf{k} = k(1, \lambda)$ and the depth contours. The remaining terms may be integrated directly to give $\psi^{(2)}$, the bounded correction to the wave function. The solution is a long wave of ψ (or pressure, or sea-surface elevation) with topographic-scale ripples on it, of relative amplitude $\sim k$ (and higher corrections $\psi^{(n)} \sim k^n$). This means that the velocity, and hence the energy, is about equally shared between the long and short scales.

The frequency is of the same order as with isolated topographic features of the same height, and does not depend on the wavelength, however great. The group velocity $\mathbf{C}_g$ is therefore at right angles to $\mathbf{k}$:

$$\mathbf{C}_g \equiv f\nabla_{\mathbf{K}}\omega = (f\delta/2\tfrac{1}{2}K)\sin\theta\,(-\sin\theta, \cos\theta),$$
$$K^2 = k^2(1+\lambda^2).$$

A slight rotation of $\mathbf{k}$ towards the depth contours raises the frequency, and this is the sense of the group velocity vector. Its magnitude is greatest when it lies along the depth contours ($|\mathbf{C}_g| = (f\delta/2\tfrac{1}{2}K)\sin\theta$), analogous to the role of the horizontal with internal waves in a non-rotating stratified fluid. In this limit the frequency vanishes, showing how a geostrophic flow along contours would penetrate at a rate $\sim f\delta L$ away from a slowly moving source of energy, L being the characteristic scale of the source. This sort of blocking effect and its similarity to the Taylor column has been described elsewhere (Lighthill 1967; Rhines 1969).

The bottom slopes vanish in the mean and it is at first sight surprising that their effects do not cancel in the limit of infinite wavelength (or, equivalently, infinitely fine-grained topography). The stretching of vortex lines, however, becomes relatively more powerful in the same limit, and the opposing tendencies just balance.

This system is thus capable of rapid energy transmission, for it supports very long waves. The large group velocities are, however, entirely due to the anisotropy of the medium; with topography that is statistically isotropic, the propagation is likely to be far less efficient.

A physical interpretation

The mechanism by which two very different scales of motion interact to produce a wave may be seen by re-examining the perturbation sequence. Consider an initial displacement Ξ of the fluid in the y direction, normal to the depth contours. Fluid moving through changing depth alters its vorticity by an amount $d\zeta \sim f\delta\Xi/a$, producing a small-scale pattern of velocity, to the right at the peaks and to the left in the troughs (figure 2*a*). Alternatively, one may think of the effect of the increasing Coriolis force on fluid accelerated (by continuity) as it moves up a slope. Note that these new long-slope velocities have no coherence on scales larger than that of the corrugations, a.

If, now, the initial displacement is made to vary gradually in magnitude (i.e. on a scale k^{-1}) in the x direction, the induced vorticities will do the same, reversing

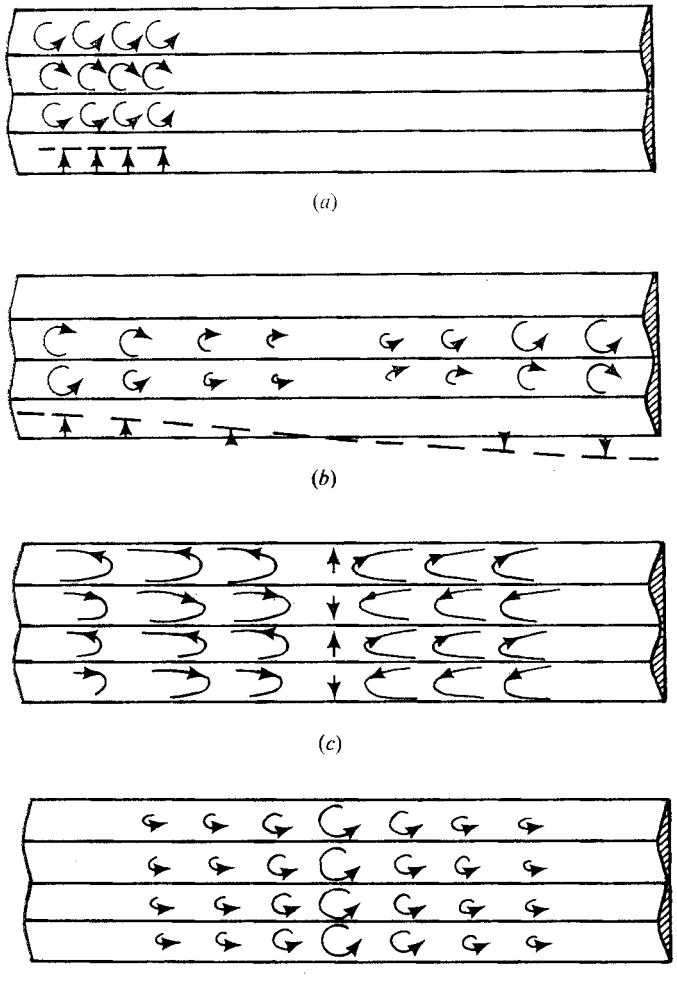

FIGURE 2. Schematic of oscillations over a sinusoid. (*a*) Vorticity due to an imposed displacement Ξ. (*b*) Effect of varying Ξ along contours. (*c*) Velocities corresponding to this pattern. (*d*) Large-scale vorticity induced by velocities in (*c*), opposite in sense to the original displacement.

in sense over a half-wavelength of the Ξ variation (figure 2*b*). These opposing vorticities induce new flow downhill, off the ridges, *everywhere* near the node of Ξ (figure 2*c*). The downhill speed v is $O(kf\delta a\Xi)$ and stretches the vorticity in a broad region at a rate proportional to Ξ (figure 2*d*):

$$d\zeta/dt = O(f\delta v/a) = O((f\delta)^2 k\Xi).$$

This gives an acceleration

$$d^2\Xi/dt^2 = -O(f^2\delta^2\Xi)$$

in response to a displacement, which is the essence of a wave.

Numerical verification

The problem was also solved numerically on a CDC-6600 computer, by integrating the finite-difference form of the vorticity equation on a 64×64 grid. An initially sinusodial pattern of velocity, directed straight across the depth contours, was allowed to evolve freely in time. A smooth periodic oscillation, figure 3 (*b*) (plate 1), then occurred, and ran for many cycles with gradual viscous decay. The topography for this run, figure 3 (*a*) (plate 1), was a sinusoid of wavelength one eighth of the width of the domain. The boundary conditions were periodic in both directions, making the geometry infinite, in effect. The frequency ω was $0{\cdot}66\delta$, compared with $2^{-\frac{1}{2}}\delta$ from the theory. A 7% discrepancy is acceptable, since the small parameter of the theory, a/L, was equal to $\frac{1}{8}$. Runs for shorter waves, $a/L = \frac{1}{2}$, were surprisingly similar to those for $a/L = \frac{1}{8}$, even though the long-wavelength theory is not then formally valid. (The frequency dropped to $0{\cdot}64\delta$ in that case, but the oscillations were still 'pure'.)

Figure 3 (*c*) shows the initial streamline pattern, representing flow towards the bottom of the page in the centre and flow towards the top at the sides of the figure. Just after the beginning of the sixth wave period, figure 3 (*d*) shows the deflexions caused by vortex stretching. By figure 3(*e*) (plate 2) the motion has shifted entirely to the topographic scale, but these eddies gang up and form a purely large-scale motion opposite to the initial one (figures 3*f*, *g*); the mean flow averages to zero. Figure 3 (*h*) shows the mid-point of the period. The relation of figure 3 to figure 2 should be quite clear.

It is interesting that, when the experiment was repeated, but including the nonlinear terms neglected in the theory, the results were substantially the same until the fluid particles were set off fast enough to surmount a ridge or trough completely. Solutions for very large initial velocities resemble simple meandering flows, with a non-vanishing mean component across the contours. At intermediate amplitudes, when the solutions are still waves, a mean Lagrangian drift of particles occurs along the contours, in accord with the theorem of Moore (1970). Further computer experiments have been assembled into a movie.

Slight generalization

The calculations are readily repeated with several Fourier components of the depth $h(y)$ present. The result analogous to (2.4) is just

$$\omega^2 = \delta^2_{\text{r.m.s.}} \cos^2\theta,$$

depending only on the root-mean-square roughness height. The convergence worsens as the number of components is increased, however, and if the analysis is attempted with $h(y)$ a stationary random function, it fails. To see this, consider the successive corrections $\psi^{(n)}$, which involve repeated integrals of $h(y)$. The first, $\psi^{(1)}$, is proportional to

$$\int_0^y h(y^1)\,dy^1 + c_1 y + c_2.$$

The linear term will cancel the dominant part of the integral if $c_1 = -H$, the mean depth. The remainder, however, is also divergent; it is like the displacement at

time y due to a random walk with speed $h(y)-H$, which diverges like $(y/a)^{\frac{1}{2}}$, where a is the correlation length of the topography.

The effect of β

With a smoothly sloping bottom, or β-effect, simple Rossby waves will compete with these solutions. Their two frequencies, $\sim \delta$ and $\sim L/R$, respectively ($R = R_e \tan$ (latitude) where R_e is the radius of the earth), are a measure of the strength of restoring forces, and the nature of the solutions should thus depend on the size of $\delta R/L$.

Let us scale the effects to have equal stature, $\delta R/L \sim 1$ (which is *not* the same as saying that the bottom slopes are comparable with the equivalent-β slope H/R; they may be much steeper). Now the scheme already developed had $\delta \sim k \equiv a/L$, the ratio of topographic to wave scales, so that

$$L/R \sim k$$

and the *same* expansion parameter k describes both the modelling of the sphere by its tangent plane and also the separation of topographic and wave scales.

The previous equations need only be slightly modified. Suppose that the corrugations run east and west. Then the northward advection of planetary vorticity, and the variation of f alter (2.2) to read

$$\hat{\psi}_{yy} - \delta \cos y \hat{\psi}_y - \left(k^2 + \frac{\delta k}{\omega}\left(1 + \frac{ay}{R}\right)\cos y\right)\hat{\psi} - \frac{ak}{\omega R}\hat{\psi} = 0,$$

where, now,

$$\omega = \sigma/f_0, \quad f = f_0(1 + ay/R),$$
$$R = R_e \tan (\text{mean latitude}).$$

The variation of f with latitude $\sim ay/R \sim k^2 y$ is only $O(k)$ over a wavelength. The final, '$\beta\psi_x$', term $\sim a/R \sim k^2$, so that we again obtain the first two of equations (2.3). The third, $O(k^2)$, equation becomes

$$\psi^{(0)}_{YY} + \left[\frac{1}{2}\frac{\delta^2}{\omega^2} - 1 - \frac{a}{\omega k R}\right]\psi^{(0)} = -\psi^{(2)}_{yy} + \psi^{(0)}_{Y}\left[2\frac{\delta}{\omega}\sin y + \frac{\delta}{k}\cos y\right]$$
$$+ \psi^{(0)}\left[-\frac{\delta^2}{2\omega k}\sin 2y - \frac{\delta^2}{2\omega^2}\cos 2y - \frac{\delta a k y}{\omega k^2 R}\cos y\right].$$

All coefficients are order unity. The left-hand side is a function of Y alone, and must vanish by itself. The right-hand side gives the $O(k^2)$ corrections to ψ. Note that the last term leads to a mild divergence over many wavelengths. This is a familiar problem with β-planes, and should not destroy the local correctness of the result. One may, as alternatives, include more stretched y-scales or retreat to an equivalent-slope model.

The large-scale behaviour has wavelike solutions

$$\psi^{(0)} = \exp i(kx + ly - \omega f_0 t),$$

with dispersion relation

$$\omega^2 + \frac{ak}{R(k^2+l^2)}\omega - \frac{1}{2}\frac{\delta^2 k^2}{k^2+l^2} = 0 \tag{2.5}$$

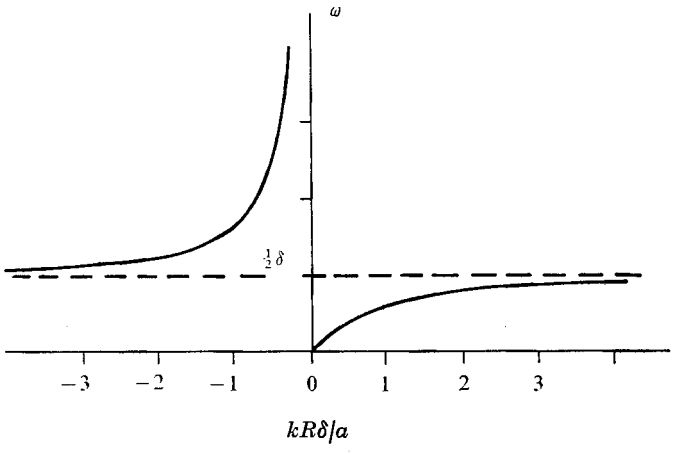

FIGURE 4. Dispersion relation for long waves ($L \gg a$) over a sinusoidal bottom, including the β-effect, $k = l$, showing the transition from Rossby to 'roughness' waves.

(reorienting the depth contours to lie at an angle α from east merely alters the middle term to

$$\left[\frac{a}{R}\frac{k\cos\alpha - l\sin\alpha}{k^2+l^2}\right]\omega,$$

where k and l are wavenumbers along and across the slope, respectively).

Figure 4 shows the dispersion relation (2.5) with k set equal to l, to show the effects of scale rather than anisotropy. The left-hand curve crosses from the Rossby to the topographic asymptote where the frequencies due to those effects taken separately are equal, that is, where

$$\delta R/L \sim 1, \quad \omega \sim \tfrac{1}{2}\delta$$

as anticipated.

Forced waves

Suppose that a wind-stress curl $(\nabla \times \boldsymbol{\tau})_z$ of large scale drives the vorticity equation, with the bottom corrugated and f again a constant. For a single Fourier component

$$(\nabla \times \boldsymbol{\tau})_z/\rho_0 = A \exp i(kx + lY - f\omega_0 t)$$

the right-hand side of (2.2) becomes

$$a^2 A\, e^{ilY}/f\omega_0,$$

with $l = O(1)$. The rule that, at each order in the two-scale expansion, $\psi^{(n)}$ must be bounded as $y \to \infty$ with Y fixed prevents the forcing term from appearing until the third, $O(k^2)$, equation of (2.3). Then the slowly varying part of the equation becomes

$$\psi^{(0)}_{YY} + \frac{1}{2}\left(\left(\frac{\delta}{\omega_0}\right)^2 - 1\right)\psi^0 = \frac{a^2}{f\omega_0} A\, e^{ilY},$$

which has a familiar resonance structure:

$$\psi^{(0)}(Y) = \frac{a^2 A\, e^{ilY}}{f\omega_0[\frac{1}{2}(\delta/\omega_0)^2 - (l^2 + \frac{1}{2})]},$$

with $\psi^{(1)}$ related to $\psi^{(0)}$ as before. This illustrates the direct shortening of length scale that occurs between the forcing function and the response; the topographic-scale velocities due to $\psi^{(1)}$ are of the same order as the large-scale velocities unless the system is being forced far from resonance.

Waves with the scale of the topography

The perturbation scheme accounts for both large- and small-scale depth variations, but the intermediate scales are also important. Indeed, in weak scattering problems, these are dominant. They lead to the analogue, over continuous topography, of the lower-mode trapped waves found with idealized, isolated seamounts and steps. In a sense they are again the 'gravest' modes, having the highest possible frequencies, and seem to make the most efficient use of the bottom bumps by mimicking their horizontal scale.

Detailed solutions are, of course, intricate. We continue to consider sinusoidal corrugations, for which (2.2) is a Mathieu equation (accepting errors of order δ). For simplicity we take $\beta = 0$, leaving

$$g_{zz} + (p - 2q\cos 2z)\, g = 0,$$

where

$$p = -4\hat{k}^2, \quad q = 2\hat{k}\delta/\omega, \quad z = y/2a, \quad \hat{k} = ka,$$
$$h = H(1 + \delta \sin y/a), \quad \delta \ll 1,$$
$$\psi = g(z)\, e^{i(kx - \omega f_0 t)}.$$

A dispersion relation may be constructed for all wavelengths, thus incorporating our earlier perturbation results. The nature of the solutions is determined by the values of p and q. In the shaded portions of figure 5 (normally called the stable region), g has wavelike solutions in z, $e^{i\nu z}P(z)$, where P gives the local structure, being periodic with period π or 2π. Elsewhere in the figure (the 'unstable' region) no solutions are found that remain bounded in $|z| < \infty$. The divergent solutions represent parametric instability in problems where z represents time, but no such interpretation is valid here.

The dispersion curves are found by fixing $\hat{k}$, thus defining a locus $p =$ constant (< 0) on figure 5. Contours of ν are plotted in the shaded bands (see standard works like McLachlan 1947, p. 98). By moving along the locus marked A we can read off q, and hence the frequency, as a function of wavenumber, but it is clearer if the total wavenumber vector $(\hat{k}, \frac{1}{2}\nu)$ is held in the same direction while its modulus is varied. Fix the propagation direction at, say, 45° relative to Oz ($\hat{k} = \frac{1}{2}\nu$) and allow ν to increase from zero, following locus B, figure 5. The resulting dispersion curve, figure 6 (a), shows little variation for the longer waves. Thus the estimate $\omega \sim \delta$ holds, rather remarkably, for all scales greater than that of the topography. The asymptotic result for long waves

$$\omega^2 = \delta^2 \frac{1 + 4(\frac{1}{6}\pi^2 - 1)\,\hat{k}^2}{2 + \nu^2/2\hat{k}^2}$$

is also plotted (dashes). Obtained from standard Mathieu formulae, it gives the first correction to the perturbation theory.

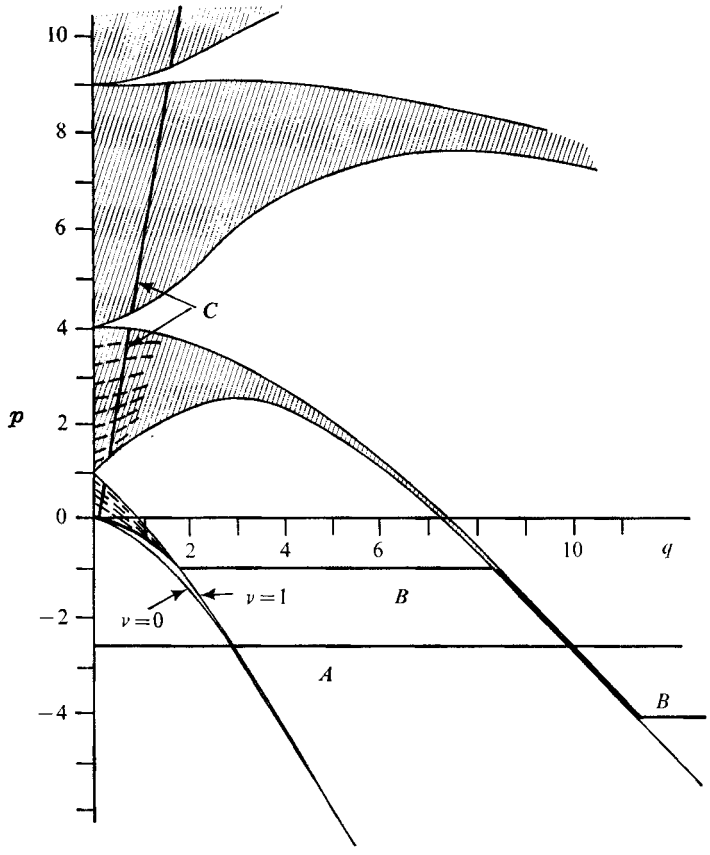

FIGURE 5. Mathieu chart for constructing the dispersion relation of waves over a sinusoid (figure 6*a*). p and q are functions of frequency and the long-slope wavenumber $\hat{k}$. Propagating solutions are found in shaded regions. Along locus A, $\hat{k}$ is fixed and the upslope wavenumber $\frac{1}{2}\nu$ is read off as a function of q (hence ω). (ν is contoured with dashed lines.) Along B the angle of propagation is fixed. C is the locus one would follow if β were included and topography slight.

At $\nu = 1$, where the wavelength is twice that of the corrugations, we run off the shaded limb on locus B, and must climb to the next one; the frequency changes drastically. Each time ψ gains another zero over one cycle of topography, the frequency drops to a lower level. The dispersion curve thus shifts from a continuous spectrum to a discrete spectrum of locally trapped oscillations, familiar in the quantum-mechanical band theory of crystalline solids. If β is retained and k fixed one follows loci like C, figure 5, to construct the dispersion curve. The particular case shown represents a slight topographic perturbation to simple Rossby waves (see Rhines 1970*b*).

The form of the z dependence of the stream function (or, approximately, the free-surface elevation) is sketched in figure 6 (*b*). It is apparent that only for very small, or very large, ν is it sensible to attribute to the motion a definite wavenumber. For very short waves a WKBJ/Airy solution can be constructed for each trough, representing the guiding of rays along contours of depth. If we had

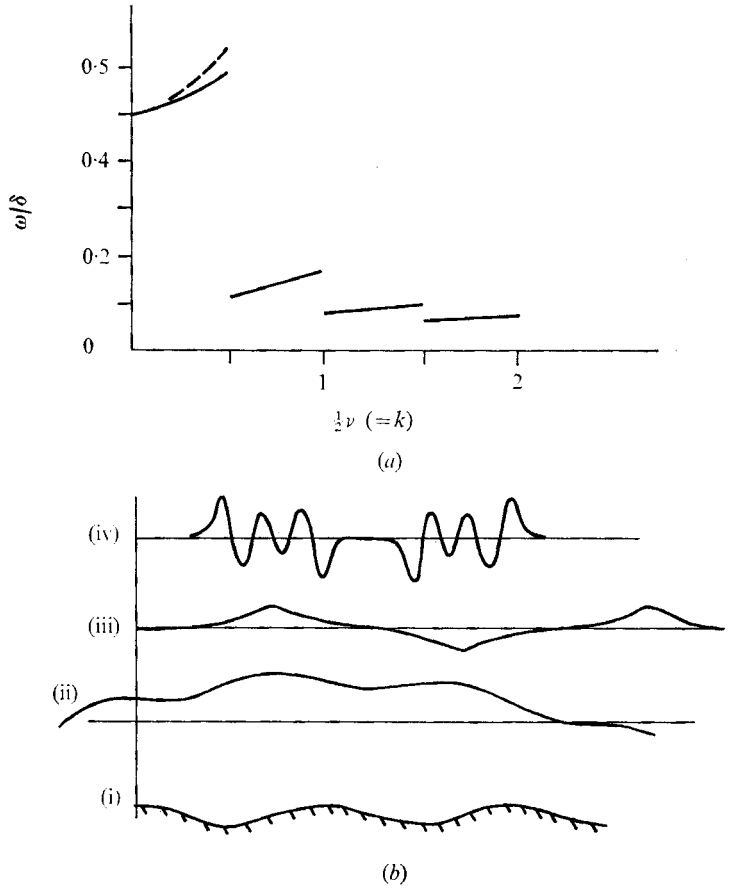

FIGURE 6. (*a*) Dispersion relation over a sinusoid, arbitrary wavelength, constructed from figure 5, locus B; $k = \frac{1}{2}\nu$. Note small change in frequency for wavelengths greater than twice that of the bottom, large changes elsewhere. (*b*) Examples of the dependence of ψ on y (it is purely sinusoidal in x) for (ii) $\nu \ll 1$, (iii) $\nu \sim 1$, (iv) $\nu \gg 1$. (i) Underlying topography.

only a half-cycle of the sinusoidal bottom, such that the slope were of one sign and joining two featureless plains, the solutions would be appropriate to trapping in a single potential well. With k fixed, ω would take on a discrete set of values corresponding to integral jumps in the wavenumber.

Now how do the adjacent ridges and troughs alter the shorter trapped waves? If ν differs only slightly from an integer, for instance, $g(z)$ is a series of potential-well oscillations, very slowly modulated in space. ω changes slightly within each zone $n \leqslant \nu < n+1$ and $\partial\omega/\partial\nu$ gives the rate at which the modulation moves across the topography. Thus the slight change in frequency within each band represents the leakage from one well to the next. The normal modes may be combined in physically interesting ways. Those corresponding to $\nu = n$ and $\nu = n+1$, for example, are Mathieu functions which are even and odd, respectively, about $z = \pi$. When added they form, initially, a potential-well solution in every *second* well, with intervening regions quiet. As time goes on this pattern disappears, reappearing in the adjacent empty wells.

In this limit the theory is a clumsy way of describing the leakage of energy through the potential barriers. A perturbation scheme based on the weakness of the coupling between wells produces the slowly modulated solutions more readily.

This example has shown a limiting behaviour of refractive trapping, of smooth long-wave propagation over roughness, and a sort of 'gravest' mode in between, which is, like the short waves, quite immobile. Despite an idealized nature it illustrates those solutions with $L \sim a$ that are likely to be the most vigorous over a bed of complex hills and valleys, and suggests how small the energy propagation is then likely to be.

3. Three-dimensional topography

Some of the previous results carry with them implications about the more difficult case of curved depth contours. The group velocity for long waves, $L \gg a$, owed its existence entirely to the anisotropy of the sinusoidal bottom: rotation of the wave crests altered the frequency. If similar long waves were to exist over isotropic roughness, their group velocity might thus be far smaller. Also recall that the frequency due to a small-scale sinusoid ($L \gg a$) and the frequency due to 'undulations', of scale $a \sim L$, were nearly the same, $\omega \sim \delta$. In a crude way, this also says that the group velocity should be small, for the dependence of frequency on wavelength over this broad range of scales is so very small. It also suggests that the response frequencies of an ocean with a very rough bottom may be quite insensitive to the initially imposed scale of the currents, if it is smaller than $\sim \delta R$ and hence out of the range of β. The horizontal scale of the roughness itself appears to be relatively unimportant to the resulting oscillation frequency (but it does control the scale of the currents).

The most misleading feature of the model with a sinusoidal bottom is probably its ability to support waves of scale large compared with that of the topography. Evidence against the existence of such long waves over three-dimensional topography is the failure of the long-wave perturbation theory (§ 2) for even a simple tessellated pattern of depth contours. The smooth channels of communication afforded by the straight ridges and troughs are no longer present, and no slight perturbation of a long wave satisfies the equation. The scale of ψ must be at least as small as that of the roughness, until β or broader slopes become dominant (further support appears in the following subsections; the implications for the energy flux of this smallness of the motion scale will be discussed).

Slight three-dimensional roughness

One analytical approach is to make the roughness inferior to slopes or β, and consider the scaling $(L/R)^2 \ll \delta \ll L/R \ll 1$ rather than the previous case of equal strength, $\delta \sim L/R$. Supposing that

$$\psi = \psi^{(0)} + \delta\psi^{(1)} + \ldots,$$

(2.1) becomes

$$\begin{aligned} \mathscr{L}\psi^{(0)} &= 0, \\ \mathscr{L}\psi^{(1)} &= (i\omega f_0)^{-1}(\nabla\psi^{(0)} \times \nabla(f/h)) \,.\, \hat{\mathbf{1}}, \\ &\vdots \end{aligned}$$

where $\mathscr{L} = \nabla^2 + (i\omega R)^{-1}\,\partial/\partial x$. Now in this limit the various Fourier components of the depth may be treated individually, then superimposed. With the bottom profile again being $h = H(1+\delta \sin y/a)$, and

$$\psi^{(0)} = A \exp i(kx + ly - \omega^{(0)} f_0 t), \quad \omega^{(0)} = -k/R(k^2+l^2),$$

we find

$$\psi^{(1)} = \frac{k}{\delta\omega}\left[\frac{\exp i[kx+(l-a^{-1})y-\omega f_0 t]}{k^2+(l-a^{-1})^2+k/\omega R} + \frac{\exp i[kx+(l+a^{-1})y-\omega f_0 t]}{k^2+(l+a^{-1})^2+k/\omega R}\right], \ldots .$$

When the denominators vanish this ordering breaks down, and a resonant interaction theory (Rhines 1970*b*) shows how two Rossby waves of the same frequency trade energy back and forth, via a catalytic Fourier component of depth, in a time of order $(f\delta)^{-1}$. If, on the other hand, $ka \gg 1$, small corrections to ψ and the frequency exist. The sizes of these corrections are, as might have been anticipated from § 2,

$$\psi^{(0)} \sim 1, \quad \delta\psi^{(1)} \sim \frac{\delta R}{L}\frac{a}{L}, \quad \delta^2\psi^{(2)} \sim \left(\frac{\delta R}{L}\right)^2 \frac{a}{L}, \ldots .$$

The appropriate small parameter for this procedure is thus $\delta R/L$, which, as before, is not the same as the ratio of topographic to equivalent-β slope. This perturbation approach can only yield a slight distortion of the large-scale streamlines, meaning that the conclusion by Robinson & Stommel (1959), that roughness greatly intensifies the currents due to an imposed Rossby wave and that the Rossby wave can even then propagate intact, is invalid. They made use of this same perturbation scheme, but introduced errors by taking the depth to be a complex function of x and y, and misjudging the size of the correction terms. It is important to observational work to know this: if a field of small (say $L \sim 50$ km wide) eddies is found, which submit to the assumptions of this sort of theory, our arguments imply that they cannot be a long Rossby wave in disguise. Specifically, our earlier discussion of the length scales implies that the energy flux due to such eddies should not greatly exceed $\mathscr{E} f \delta L$ ($\mathscr{E}$ being the energy density).

At the second order in the above perturbation sequence a frequency correction must be made, analogous to the self-interaction or 'Stokes' correction. It reveals the first change in the group velocities. Without presenting the details, which are straightforward, the result for isotropic roughness is

$$\omega = \omega^{(0)}(1 + \delta^2_{\text{r.m.s.}}/2\omega^{(0)2}),$$

where ω_0 is the uncorrected Rossby frequency and $\delta^2_{\text{r.m.s.}}$ the variance of the depth. This agrees with the superposition of earlier results. The formula already shows a reduced group velocity, equal to

$$fL\left(\frac{\partial\omega^{(0)}}{\partial k}, \frac{\partial\omega^{(0)}}{\partial l}\right)(1 - \delta^2_{\text{r.m.s.}}/2\omega^{(0)2}).$$

An exact solution

The analysis for continuous three-dimensional depth profiles is so difficult that it seems worthwhile to present a simple solution even though the shape of the topography is rather peculiar. It provides more fuel for arguments against the ability of rough topography to transmit energy quickly.

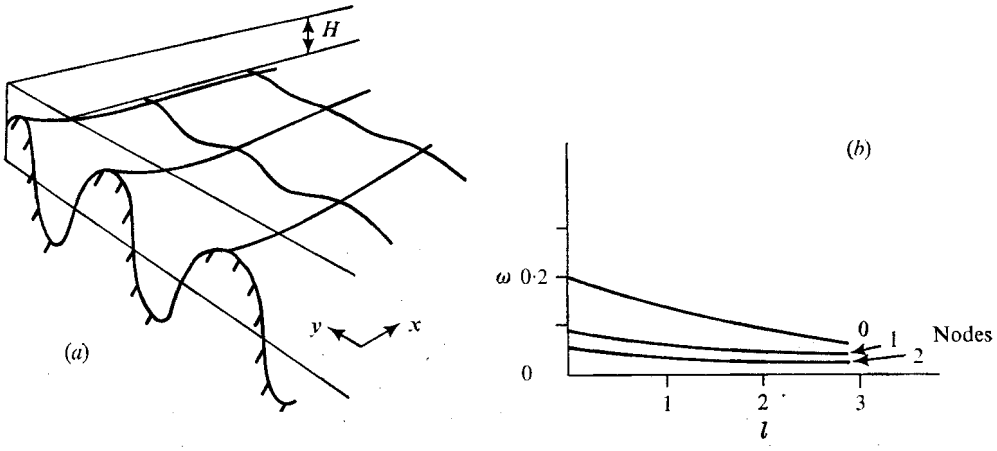

FIGURE 7. (*a*) The bottom profile $h = H\exp(e^{-x}\sin y)$, $x \geqslant 0$. (*b*) The dispersion relation for waves over the above profile. l is the y wavenumber. The number of nodes parallel to the coast is indicated.

Equation (2.1) can, for a special class of topography, be reduced to a membrane vibration problem. If f is a constant, (2.1) becomes

$$\nabla^2\phi + p(x,y)\,\phi = 0$$

as long as $h(x,y)$ satisfies

$$\nabla^2\tilde{h} = 0, \quad \tilde{h} = \ln h.$$

The dependent variables are related by

$$\psi = \left[h^{\frac{1}{2}}\exp\left(-\frac{i}{2\omega}\int\tilde{h}_y\,dx + a(y)\right)\right]\phi(x,y) = \left[h^{\frac{1}{2}}\exp\left(\frac{i}{2\omega}\int\tilde{h}_x\,dy + b(x)\right)\right]\phi(x,y),$$

where the functions of integration $a(y)$ and $b(x)$ are chosen to make the two expressions equal. The new coefficient is

$$p = \tfrac{1}{4}[(\omega^{-2}-1)\,|\nabla\tilde{h}|^2]$$

(if the term $\nabla h^{-1}.\nabla\psi$ is neglected in (2.1), yet β retained with f held constant, a similar reduction is possible). The substitution is akin to the familiar procedure that removes the first-derivative term from a second-order ordinary differential equation. Since harmonic functions are not a complete set, the reduction is far from being a general one.

We choose the depth dependence

$$h = H\exp(e^{-x}\sin y),$$

representing large undulating variations in depth in $x < 1$. At $x = 0$ the range of h is $2{\cdot}35H$, but as $x \to \infty$ the bottom becomes flat (figure 7*a*).

Since $|\nabla\tilde{h}|^2 = e^{-2x}$ the equation becomes separable:

$$\nabla^2\phi + |\tfrac{1}{4}(\omega^{-2}-1)\,e^{-2x}|\,\phi = 0.$$

The solutions are of the form

$$\phi = e^{ily}\,\mathscr{C}_l(\kappa e^{-x}),$$

where

$$\kappa^2 = \tfrac{1}{4}(\omega^{-2}-1)$$

and $\mathscr{C}_l(z)$ is one of the solutions of Bessel's equation. The stream function has unbounded variation as $x \to -\infty$, so we exclude the left half-space with a 'coast' at $x = 0$, on which ψ vanishes. Then the physical domain corresponds to the interval

$$0 \leqslant z < \kappa, \quad z = \kappa e^{-x}.$$

The full solution is then

$$\psi = AB,$$

$$A = h^{\frac{1}{2}} e^{-i\tilde{h}_y/2\omega}, \quad B = e^{ilY} J_l(\kappa e^{-x}),$$

$$\tilde{h}_y = e^{-x} \sin y, \quad \omega^2 = 1/(4\kappa^2 + 1).$$

With the boundary condition $J_l(\kappa) = 0$, the dispersion relation is determined, as shown in figure 7 (b). As with ordinary edge waves the modes are distinguished by the number of nodes parallel to the coast. The limit $l \to 0$ gives the highest frequency ($\omega = 0{\cdot}20$), even though the topography has a small horizontal scale. The function A varies on the topographic scale, while the y dependence of B may occur on any scale. This happened also with oscillations over a corrugated bottom, but here the variation on the topographic scale is much stronger; near the 'coast' the variations of A almost obscure those of B.

In spite of the complex shape of the eigenfunctions, the quantity $\partial\omega/\partial l$ does have meaning as a propagation velocity of energy along the coast. The greatest value occurs for $l \to 0$, at which point $\partial\omega/\partial l \simeq -0{\cdot}12$ (energy and phase always move in the sense of a Kelvin wave). This is of the same order as $\omega \times$ scale of topography, rather than $\omega \times$ wavelength, indicating that in an energetic sense no long waves are possible in this system. The scale estimates of frequency ($\omega \lesssim \delta$) were intended for small deviations from the mean depth, $\delta \ll 1$. Nevertheless, $\frac{1}{2}\delta$ from this topography is about 0·4 at the coast, and vanishes for large x; the waves seem thus to average the topographic heights beneath them, in selecting their natural frequency.

Bounds and estimates for the frequencies

It is shown in the appendix that, for arbitrary bottom topography, the set of quasi-geostrophic waves $\hat{\psi}(x, y)\, e^{-i\omega f_0 t}$ in a basin closed by vertical walls form an orthogonal set. In practice, the calculation of the response to wind stress by decomposition into normal modes is viable only with smooth slopes, or not at all. Here, with a very rough bottom, the eigenfunctions will have complicated spatial structure which is very sensitive to the exact eigenfrequency, and owing to their inefficient energy-carrying properties, these modes may be difficult to excite in totality.

Nevertheless, the variational principle (A 2) is revealing. Taking $\beta = 0$, (A 2) becomes

$$\omega < |h(f/h)|_{\max}.$$

To $O(\delta)$ this is

$$\omega \leqslant |h - H|_{\max}/H,$$

where H is the mean depth. Including β the analogous result is

$$\omega \leqslant \left| \frac{f - f_0}{f_0} - \frac{h - H}{H} \right|_{\max}$$

to $O(\delta) + O(L/R)$.

This upper bound agrees closely with the actual frequencies encountered in the special cases above, and also with abrupt topographic ridges, steps and seamounts. It is evidence that there is indeed some insensitivity of the natural frequencies of response to the precise horizontal structure of the bottom.

A number of computer experiments have been performed by Rhines and assembled into a movie. These show linear waves over topography of varying complexity, and give further weight to the estimate $\omega \sim \delta$, where δ is rather locally determined (and not globally averaged), to the slowness of energy propagation over roughness, and to quantifying the view, discussed below, that the fluid participates in a wavenumber cascade from small, initially imposed, wavenumbers to those of the dominant bottom roughness.

Weakly-coupled seamounts

We have not yet exhausted the analytical possibilities. An approach (given here in outline only) can be made by starting from a set of normal modes representing oscillations trapped about individual seamounts and islands. If the features are sparsely distributed (say an average distance D apart) on an otherwise flat bottom, the coupling parameter $a/D \ll 1$, where a is now the typical seamount radius, and a perturbation expansion in a/D is sensible. With Rossby waves present this resembles the problem (Rhines 1969) of scattering from isolated potential wells; it gives another illustration of conversion of large-scale incident energy into small-scale oscillations (and resonances are possible, for which the topographically induced currents are stronger than those of the Rossby wave that created them, but the relevance of such resonances to the ocean remains moot).

If we restrict the fluid length scales to be small, however, Rossby waves will locally be subordinate to an f-plane effect, the gradual leakage of energy from one seamount to the next. The full equation, neglecting β, is

$$\nabla . (h^{-1} \nabla \psi_t) - f(\nabla \psi \times \nabla h^{-1}) . \hat{\mathbf{i}} = 0.$$

For instance, if

$$h(x, y) = H(1 + \delta \Sigma A_i \hat{h}_i(x, y)), \quad \delta \ll 1,$$

where the $\hat{h}_i$ are a random set of seamounts,

$$\hat{h}_i = \begin{cases} 1 - [(\mathbf{r} - \mathbf{r}_i)/a_i]^2, & |\mathbf{r} - \mathbf{r}_i| \leqslant a_i, \\ 0, & |\mathbf{r} - \mathbf{r}_i| > a_i, \end{cases} \quad \mathbf{r} \equiv (x, y),$$

then the first approximation is a set of independent oscillations:

$$\psi = \Sigma B_i \psi_i \quad (B_i \text{ arbitrary}),$$

$$\psi_i = \begin{cases} \sum\limits_{s<0} \exp(is\theta_i - \omega_{is} f_0 t) J_s(\alpha_{is} r_i)/J_s(\alpha_{is} a_i), & r_i \leqslant a_i, \\ \sum\limits_{s<0} \exp(is\theta_i - \omega_{is} f_0 t) (r_i/a_i)^{-|s|}, & r_i > a_i, \end{cases}$$

where (r_i, θ_i) are polar co-ordinates centred on the ith seamount. The eigenvalues α_{is} allow the matching of velocity components at $r_i = a_i$. The corresponding eigenfrequencies densely populate $\omega \leqslant \delta$ (Rhines 1969):

$$\omega_{is} = -2\delta_i s/(\alpha_{is} a)^2,$$

for small paraboloidal seamounts. Now at the next order in a/D the oscillation at the ith seamount is felt by its nearest neighbours. Suppose that all of the energy initially lay at a single seamount with $i = 1$ and $s = -1$. Then the neighbours, with $i = j$, would feel a broad, slowly oscillating current, and respond according to

$$\nabla . [h^{-1} \nabla (\partial \psi_j / \partial t)] - f_0 (\nabla \psi_j \times \nabla \hat{h}_j^{-1}) . \hat{\mathbf{i}} = f_0 (\nabla \psi_1 \times \nabla \hat{h}_j^{-1}) . \hat{\mathbf{i}},$$

where the forcing function is

$$\psi_1 = B_1 \frac{a_i}{D_{j1}} \left(1 + \frac{r_j \cos (\theta_j - \phi_{j1})}{D_{j1}} \right) \exp (-i \omega_{11} t).$$

D_{j1} is the distance between seamounts and ϕ_{j1} the bearing of the first relative to the jth. The solutions for the ψ_j show a typical resonance structure favouring lowest modes (those with $s = -1$ and the fewest nodes) and frequencies near that of the forcing. The amplitude is small, $O(a/D)$, unless the primary oscillation is at a frequency within $O(a/D)$ of an eigenfrequency of its neighbour. Then secular growth of the neighbouring oscillation occurs until it (and others like it) drains ψ_i of its energy. A computer experiment with a pair of identical seamounts showed a trading of energy back and forth, just as with weakly coupled mechanical oscillators. Clearly, energy transmission under these dynamics would resemble percolation more than propagation.

An analogous problem in solid-state physics

A wave-propagation problem with broadly similar features concerns the vibration of atomic lattices. One class of phenomena occurs when high-energy particles are projected toward a regular lattice, which is modelled as a periodic variation in the potential field. Scattering is strongest when resonance between the incident wave function and the lattice periodicity is satisfied. But these effects, which are very sensitive to the strict periodicity of the medium, normally belong in the lower part of figure 1, where weak resonant interactions occur.

In another class of problem, the atomic lattice is riddled with impurities, and may have a glass-like disorder. As we have found here, the problem is most tractable when the medium varies in one direction only. Dean (1967) discusses vibrations of one-dimensional atomic chains, in which the neglect of all but nearest-neighbour interactions leads to a simple wave difference equation, essentially a classical lumped-mass model of a vibrating string.

Figure 8, reproduced from Dean's review paper, shows the result of a computer experiment with a long (250 000 element) equally spaced chain of two atomic species mixed at random (the mass ratio of the two species is 2 : 1). The ordinate of the figure is the number density $G(\omega^2)$ of vibrational modes [of time dependence $\exp(-i\omega t)$] with respect to frequency squared, ω^2. At lower frequencies the curve is smooth, as is appropriate to long waves that average over the irregularities. There, the modes occur at equal intervals of wavenumber k and behave like $\exp(ikx)$; $G(\omega)$ is just $(\pi \omega \, \partial \omega / \partial k)^{-1}$. As the scale of the waves decreases to the order of the atomic spacing, the modal density becomes very complex. Peaks appear, corresponding to particularly likely, localized vibrations of clusters of light atoms in a heavy local environment. The spatial structure thus becomes complex, and

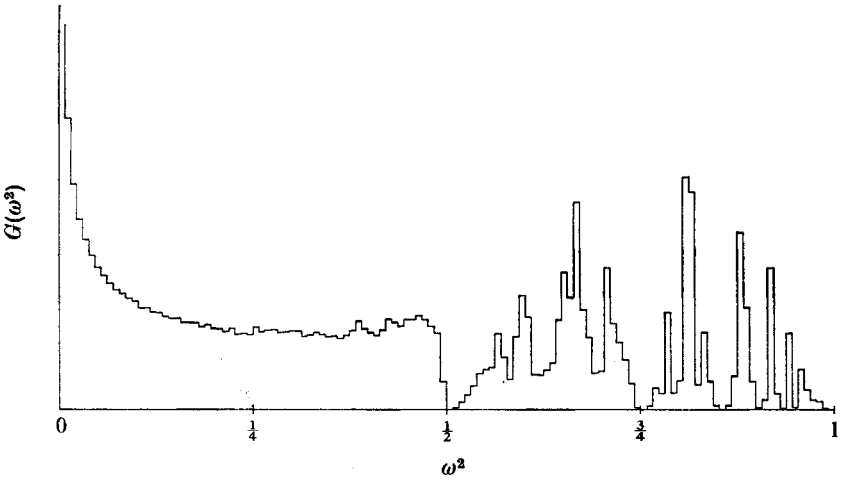

FIGURE 8. From Dean (1967), the distribution of eigenmodes with respect to frequency squared, for a long disordered chain of atoms: two atomic species present, of mass ratio 2:1. Much fine structure has been suppressed by the numerical technique.

energy propagates more slowly and less simply. Similarly, in the present problem, sufficiently long Rossby waves can exist by averaging over the irregularities in depth, while shorter waves become trapped in a small region in space. Analogous to the peaks in $G(\omega^2)$, where many modes cluster in a narrow frequency band, is the flatness of the dispersion curves in figures 6 and 7 and the attendant small group velocity (in regions where it is meaningful).

The inclusion of more than just two species of atom would blur the peaks in figure 8, but with the physical nature of the short-wave region remaining the same. If, on the other hand, the number of species were kept at two, while their mass ratios were increased, more and more of the spectrum would be occupied by 'trapped' oscillations (Domb *et al.* 1959) of light atoms 'bounded' by heavy atoms. This is the analogue of an increasingly rough-bottomed ocean.

4. Conclusions

We have illustrated the dependence of waves, initially set into motion with a length scale L, on the scale a of the depth variations. Simplifying the latter into three ranges, we called scales for which $a \ll L$ *roughness*, for which $a \sim L$ *undulations*, and for which $a \gg L$ *slope*. The β-effect in a homogeneous fluid of course acts like a slope $\simeq H/R = 0{\cdot}6 \times 10^{-3} \cot \lambda$, for a mean depth H of 4 km.

The problems treated were (*a*) two-dimensional sinusoidal 'roughness', alone, for which $\omega \sim \delta$; (*b*) a sinusoid with a slope, where the competition between Rossby waves and 'corrugation' waves was decided simply by the size of $\delta/\delta_{\text{slope}}$, δ_{slope} being the net change in depth over the wave scale L, or by $\delta R/L$ with the β-effect; (*c*) motion forced by wind stress, which yielded the usual resonance structure relative to the natural wave frequencies (the currents, as above, had about half their energy in very small eddies, demonstrating the shift

in dominant scale from that of the driving to that of the topography); (*d*) two-dimensional undulations, which again had $\omega \sim \delta$ (in a sense these oscillations wholly at the topographic scale are the gravest and most important over a very uneven bottom); (*e*) very slight, three-dimensional roughness; (*f*) an exact solution for a particular undulating sloping bottom (covering the entire range of L/a), which demonstrated that over strong three-dimensional irregularities the effective scale of the wave relevant to energy propagation is that of the topography, so that the energy velocity $\sim f\delta a$ more nearly than $f\delta\times$ (initially imposed scale of motion); (*g*) upper bounds for the frequency, which were found to be close to those in numerous analytical cases ($\omega \lesssim \delta + L/R$); (*h*) another approach to the problem of 'undulations', in which trapped oscillations about seamounts were weakly coupled; and finally, (*i*) the identification of analogous behaviour in the vibrations of irregular atomic lattices.

It is apparent that the topographic, $\mathbf{u}.\nabla h$, term raises many of the same problems as does the nonlinear $\mathbf{u}.\nabla\mathbf{u}$ term in the equations of motion. There is an analogy in that proceeding from the periphery of figure 1 to its centre (i.e. from slight or gradual, to rough topography) is rather like proceeding from the linearized theory of parallel-flow instability, say, towards the turbulent regime. In the more tractable, peripheral areas, individual Fourier components of the perturbation flow are only weakly coupled, and provide a basis for refinement, while in the central region rapid cascades of energy occur between Fourier modes. Analytically, turbulence is all the more difficult owing to the impossibility of superposing individual solutions; the present problem is bilinear; any number of solutions over the same topography are superposable, yet motion over a complex bottom is not the sum of solutions over individual Fourier components.

In the peripheral areas of the diagram the weakness of the disturbing topography (or, analogously, shear) puts an emphasis on precise tuning of the phases of the Fourier components of the flow which all but vanishes in the turbulent region, where the coupling between modes is strong and interactions cease to be selective. Scale analysis of the energy-transfer rates between Fourier components is a useful tool in turbulence (and seems to work better there, for the lack of phase sensitivity). The difficulty found with strongly coupled Fourier components leads one to search for a set of normal modes with better endurance (vortex sheets, and seamount oscillations, perhaps) but it is fair warning that the immense effort applied to turbulence theory does not seem to have advanced us far beyond the initial scale and dimensional analysis. Nevertheless, Rhines (in preparation) has attempted to view the topographic effect as a homogeneous cascade to large wavenumbers, when the depth variations have a broad spectrum, with logic analogous to an early turbulence theory of Oboukhov. This cascade moves solutions from the left-hand side of figure 1 towards is centre (one also expects generally rightward motion owing to refraction at *large* wavenumber, $ka \gg 1$, for ever smaller group velocities are associated with ever shorter waves).

The theory has provided some measure of the relative strength of 'smooth' and 'rough' propagation effects in a barotropic ocean, and may be of help in interpreting complex current-meter and float data. It is likely that the fragmentation of currents by bottom roughness is at least partially responsible for the smallness

of the observed energy-containing ocean eddies, for instance in the Sargasso Sea. There is also the implication that rough areas, like the western North Pacific, and topographic barriers, like the New Zealand Rise, may prevent Rossby-wave energy from reaching the western boundary, and hence limit the strength of the (barotropic part of the) boundary currents. The detailed results make more precise the notion that the equatorial regions, where f is small, are a smooth channel for east–west propagation. And the role of the topographic 'cascade' in providing a sink for large-scale energy is interesting, for geostrophic turbulence theory shows that turbulent dissipation by the large-scale horizontal eddies, themselves, is hard to come by.

The effects of density stratification and advection are the subject of recent work by Suarez (1971) and Rhines (1970*a*,*b*, 1971*a*,*b*, 1972). While they introduce several new effects, the results of the present work still appear relevant to geophysical flows.

We are grateful for support from the following sources: the Marshall Aid Commemoration Commission, the National Science Foundation (GX-36342) and the National Center for Atmospheric Research. Dr W. R. Holland and Dr D. K. Lilly helped with the computer experiment. Parts of this work were carried out when both authors were at the University of Cambridge.

Appendix. Integral properties

When the fluid is enclosed in a basin, (2.1) with $\psi = 0$ on the rigid vertical walls describes the normal modes $\{\psi_n\}$ corresponding to eigenfrequencies $\{\sigma_n\}$ (the vertical walls model the order-one reflexion expected at the steep face of the continental shelf). There exist the following integral properties similar to those in simpler eigenvalue problems, even though the exact ψ_n can be very complex and the σ_n very dense, for general $h(x, y)$. The utility of the normal modes, when topography dominates the motions, is in doubt, but they may describe the largest-scale oscillations of a relatively smooth ocean. In such a case the Rayleigh–Ritz procedure might be used with the variational principle given below, to study slight topographic effects. We expect, however, that it will usually be ill suited to do so.

The frequencies are real

Linearized inviscid long waves in a closed basin with a rigid lid conserve total kinetic energy, and hence the ψ_n, providing that they exist, have real frequencies. This is shown by forming $\psi^* \mathscr{L}\psi + \psi(\mathscr{L}\psi)^*$, where $\mathscr{L}$ is the operator in (2.1), and integrating over the area $\mathscr{S}$ of a basin with a lateral boundary $\mathscr{C}$. The result is $\sigma = \sigma^*$. It is of interest that the approximate equation (in the spirit of the Boussinesq approximation) for small depth changes, in which the first h in (2.1) is held constant, and f is held constant except where it is differentiated, also conserves energy exactly.

The velocities are orthogonal with respect to the weighting function $h(x, y)$

If we form $\psi_m^* \mathscr{L}\psi_n + \psi_n(\mathscr{L}\psi_m)^*$, integrate and apply $\psi = 0$ on $\mathscr{C}$,

$$-i(\sigma_m - \sigma_n)\iint h^{-1}\nabla\psi_m^* . \nabla\psi_n \, dx\, dy = \iint \frac{f}{h}[J(\psi_n, \psi_m^*) + J(\psi_m^*, \psi_n)]\, dx\, dy = 0.$$

This may be written as

$$(\sigma_m - \sigma_n)\iint h\mathbf{U}_m^* . \mathbf{U}_n \, dx\, dy = 0,$$

$$U_i = |\nabla\psi_i / h \times \hat{\mathbf{i}}|,$$

which is a simple extension of Greenspan's (1965) result for variable f.

If an initial two-dimensional field of velocity and displacement is imposed on the fluid, the formal solution can be written as the sum of normal modes, scaled in amplitude by the integrals

$$\iint_{\mathscr{S}} h\mathbf{U}_m . \mathbf{U}_m^* \, dx\, dy.$$

In addition, Greenspan (1965) has shown, for f constant, that when the depth contours are closed the steady geostrophic mode $\psi = \psi(h)$ absorbs the portion of the initial velocity with non-zero circulation about a contour. Here the geostrophic mode $\psi(f/h)$ serves the same purpose.

Variational principle for the frequencies

Such integral expressions for an eigenvalue often show that the system acts to make some physical property extreme. We form $\psi_n^* \mathscr{L}\psi_n$ and integrate, giving

$$\sigma = \frac{-i\iint_{\mathscr{S}} (f/h)\, J(\psi_n, \psi_n^*)\, dx\, dy}{\iint_{\mathscr{S}} h^{-1}|\nabla\psi_n|^2 \, dx\, dy}$$

$$= \frac{-i\iint f h\mathbf{U}_n \times \mathbf{U}_n^* . \hat{\mathbf{i}}\, dx\, dy}{\iint h\mathbf{U}_n . \mathbf{U}_n^* \, dx\, dy}, \tag{A 1}$$

where the horizontal velocity is $Rl\mathbf{U}(x, y)\, e^{-i\sigma t}$.

It may be shown, by expanding the test functions in a series of $\{\psi_n\}$, that the true frequencies are maxima of the ratio (A 1) under slight variations of ψ everywhere but on $\mathscr{C}$.

An upper bound for the highest frequency (the fundamental) now may be found. We note that contributions to the numerator of (A 1) depend on the *variations* of f/h about its mean, since

$$\int_{\mathscr{S}} J(\psi, \psi^*)\, dx\, dy = 0, \quad \psi = 0 \quad \text{on} \quad \mathscr{C}.$$

Letting f_0 and H be the mean values of $\hat{f}$ and $\hat{h}$, the fluctuations of f and h, respectively, and

$$\widehat{\left(\frac{f}{h}\right)} = \frac{f}{h} - \frac{f_0}{H},$$

it follows that

$$\begin{aligned}\sigma &= \frac{\iint \widehat{(f/h)}\, h^2 |\mathbf{U}\times\mathbf{U}^*|\, dx\, dy}{\iint h\mathbf{U}\cdot\mathbf{U}^*\, dx\, dy} \\ &\leqslant \left|h\widehat{\left(\frac{f}{h}\right)}\right|_{\max} \frac{2\iint h|\mathbf{U}_r\times\mathbf{U}_i|\, dx\, dy}{\iint h(|\mathbf{U}_r|^2+|\mathbf{U}_i|^2)\, dx\, dy} \\ &\leqslant |\widehat{h(f/h)}|_{\max} \qquad \text{(A 2)}\end{aligned}$$

since, by the triangle inequality, $2|\mathbf{U}_r|\,|\mathbf{U}_i| \leqslant |\mathbf{U}_r|^2+|\mathbf{U}_i|^2$. For small variations in f and h, this is $\sigma/f_0 \leqslant |\hat{f}/f_0 - \hat{h}/H|_{\max}$. The first term is of order L/R, where L is the size of the basin, and represents the Rossby-wave contribution. When the topography has isolated features the inequality gives a realistic upper bound, describing the trapped oscillations. The *same* bound applies to a dense field of bumps, or to waves on a slope. In no case is σ greater than $f_{\max}$.

When f is constant two physical principles follow from (A 1). The first describes the net area swept out by the particle orbits. If the displacement vector of a particle about the centre of its path is

$$\mathbf{r} = Rl\hat{\mathbf{r}}(x,y)\, e^{-i\sigma t},$$
$$\hat{\mathbf{r}} = -\sigma^{-1}(\mathbf{U}_i - i\mathbf{U}_r)$$

and then

$$\mathbf{U}\times\mathbf{U}^* = -4i\sigma[\tfrac{1}{2}\mathbf{r}\times\mathbf{U}].$$

The term in brackets is the rate at which a particle sweeps out horizontal area in time; this is independent of time, so the average area $\mathscr{A}/\iint h\, dx\, dy$ swept out in a period by the fluid particles is proportional to the numerator of (A 1):

$$\iint_{\mathscr{S}} h\mathbf{U}\times\mathbf{U}^*\, dx\, dy = \frac{-2i\sigma^2}{\pi}\mathscr{A},$$
$$\mathscr{A} = \iint_{\mathscr{S}} \frac{h}{2}\mathbf{r}\times\mathbf{U}\, dx\, dy.$$

$\mathbf{U}_r$ and $\mathbf{U}_i$ are not perpendicular in general, but the displacements may be referred to orthogonal co-ordinates x and y:

$$x = \frac{|\mathbf{U}_i|}{\sigma}\cos\sigma t + \frac{|\mathbf{U}_r|}{\sigma}\sin\sigma t\cos\phi, \quad y = \frac{|\mathbf{U}_r|}{\sigma}\sin\sigma t\sin\phi,$$

where the x axis is taken along $\mathbf{U}_i$, which is inclined to $\mathbf{U}_r$ at an angle ϕ.

Eliminating t from these equations,

$$\frac{\sigma^2[x-(\cot\phi)\, y]^2}{|\mathbf{U}_i|^2} + \frac{\sigma^2 y^2}{|\mathbf{U}_r|^2\sin^2\phi} = 1.$$

The particle paths are ellipses skewed with respect to x and y.

The square of the radius vector is

$$|\mathbf{r}|^2 = (x^2+y^2) = \sigma^{-2}(|\mathbf{U}_i|^2\cos^2\sigma t + |\mathbf{U}_r|^2).$$

Its average in time is just

$$\langle|\mathbf{r}|^2\rangle = (2\sigma^2)^{-1}(|\mathbf{U}_i|^2+|\mathbf{U}_r|^2)$$

and thus the denominator is

$$\iint_{\mathscr{S}} h(\mathbf{U}\,.\,\mathbf{U}^*)\,dx\,dy = \iint h(|\mathbf{U}_i|^2+|\mathbf{U}_r|^2)\,dx\,dy$$
$$= 2\sigma^2R^2,$$

where R^2 is the mean-square distance of the particles from their centres. The variational principle may now be written as

$$\delta\omega = 0, \quad \omega = \mathscr{A}/\pi R^2, \quad \omega = \sigma/f.$$

The frequency thus represents an 'efficiency' of the particles in sweeping out *net* area (positive orbits cancel negative ones), which the system strives to make a maximum.

It does not, however, manage very well. Regardless of the dynamics, a periodic two-dimensional field with a perfectly constant depth and rigid side walls sweeps out no net area at all, since

$$\iint J(\psi,\psi^*)\,dx\,dy = 0.$$

As shown above, $\delta_{\max}$, rather than 1, is the upper bound of σ/f.

Apart from this interpretation the integrals give an invariant which characterizes the motion. Still holding f constant, we may write (A 1) as

$$\frac{2}{f} = -\iint_{\mathscr{S}} h\mathbf{r}\times\mathbf{U}\,.\,\hat{\mathbf{1}}\,dx\,dy \Big/ \frac{1}{2}\iint_{\mathscr{S}} h\,|\mathbf{U}|^2\,dx\,dy.$$

The numerator is proportional to J, the average angular momentum of particles about their orbital centres (evaluated in the rotating system). The denominator is just T, proportional to the kinetic energy, averaged over all the particles. The invariant is thus

$$J/T = -2/f, \quad \text{or} \quad T+\Omega J = 0, \quad \Omega = \tfrac{1}{2}f,$$

a fact which could have been deduced from a more general result of Lamb (1945, §§ 203 ff).

REFERENCES

Dean, P. 1967 Atomic vibrations in solids. *J. Inst. Maths. Applics.* **3**, 98.

Domb, C., Maradudin, A., Montroll, E. & Weiss, G. 1959 *Phys. Rev.* **115**, 18.

Frisch, U. 1968 Wave propagation in random media. In *Probabilistic Methods in Applied Mathematics* (ed. Bharucha–Reid), vol. 1. Academic.

Greenspan, H. 1965 On the general theory of contained rotating fluid motions. *J. Fluid. Mech.* **22**, 449.

Lamb, H. 1945 *Hydrodynamics*, 6th edn. Dover.

Lighthill, M. J. 1967 On waves generated in dispersive systems by travelling forcing effects, with applications to the dynamics of rotating fluids. *J. Fluid Mech.* **27**, 725.

McLachlan, N. W. 1947 *Theory and Application of Mathieu Functions.* Oxford University Press. (Republ. 1964, Dover.)

Moore, D. W. 1970 The mass transport velocity induced by free oscillations at a single frequency. *Geophys. Fluid Dyn.* **1**, 237.

Rhines, P. B. 1969 Slow oscillations in an ocean of varying depth. *J. Fluid Mech.* **37**, 161–205.

Rhines, P. B. 1970*a* Edge-, bottom- and Rossby waves in a rotating stratified fluid. *Geophys. Fluid Dyn.* **1**, 273.

Rhines, P. B. 1970*b* Wave propagation in a periodic medium. *Rev. Geophys.* **8**, 303.

Rhines, P. B. 1971*a* A note on long period motions at Site D. *Deep-Sea Res.* **18**, 21.

Rhines, P. B. 1971*b* A comment on the Aries observations. *Phil. Trans. Roy. Soc.* A **270**, 461.

Rhines, P. B. 1972 Observations of the energy-containing oceanic eddies, and related theories of waves and turbulence. *Boundary Layer Met.* **4**, 345.

Robinson, A. R. & Stommel, H. M. 1959 Amplification of transient response of the ocean to storms by the effect of bottom topography. *Deep-Sea Res.* **5**, 312.

Smith, R. 1971 The ray paths of topographic Rossby waves. *Deep-Sea Res.* **18**, 477.

Suarez, A. 1971 The propagation and generation of topographic oscillations in the ocean. Ph.D. thesis, Department of Meteorology, M.I.T.

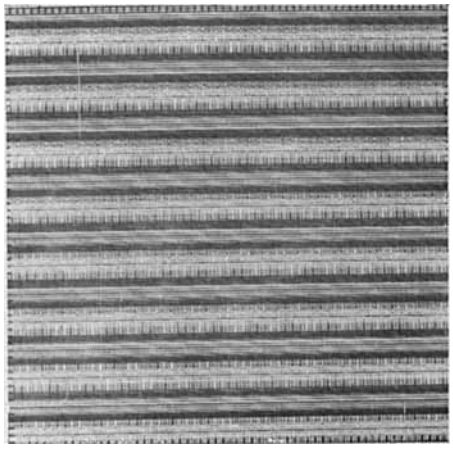

(*a*)

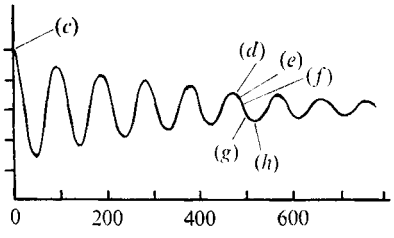

(*b*)

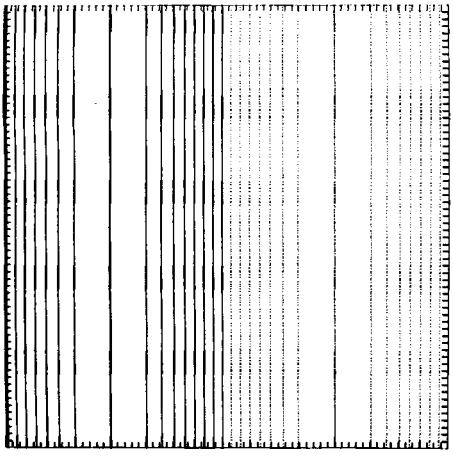

(*c*)

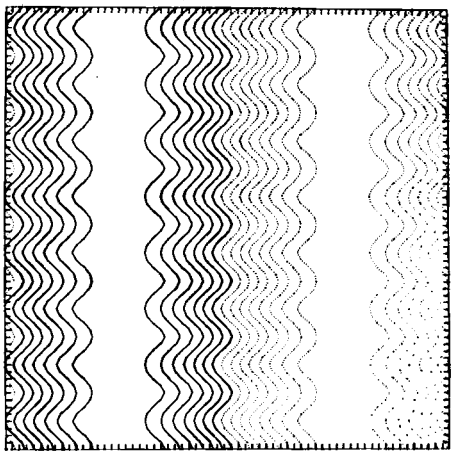

(*d*)

Figures 3 (*a–d*). For legend see overleaf.

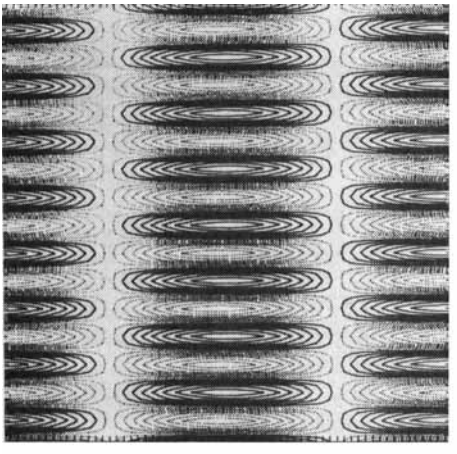

(*e*)

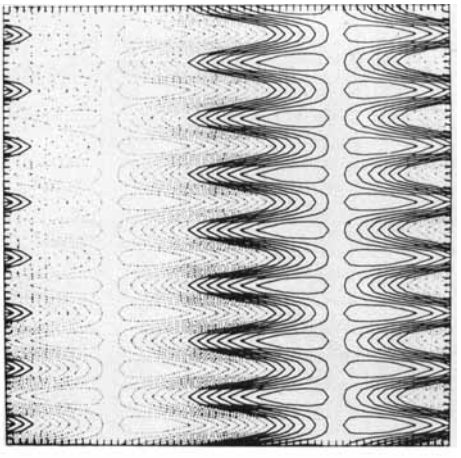

(*f*)

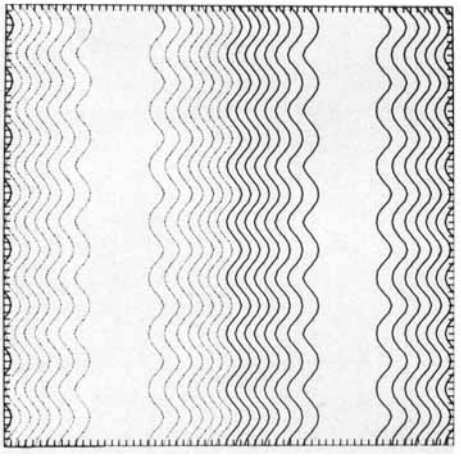

(*g*)

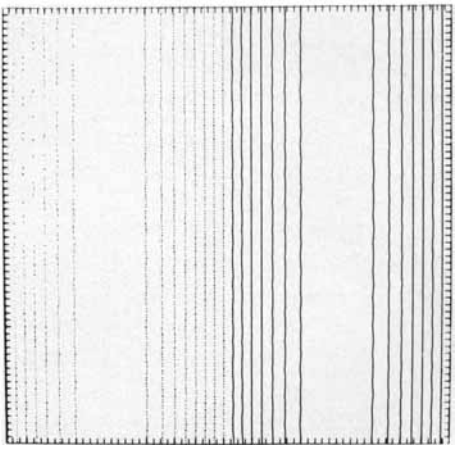

(*h*)

FIGURE 3. Reproduction, by finite-difference integration, of waves over a sinusoid. (*a*) Contours of the bottom corrugations. (*b*) ψ, or pressure, *vs.* time at a fiexd position, and orientation of succeeding parts of figure. (*c*) Initial streamlines at $t = 0$. (*d*) Shortly after beginning of fifth period ($t = 480$ arbitrary units). (*e*) $t = 490$. (*f*) $t = 500$. (*g*) $t = 520$. (*h*) $t = 530$. Solid contours are positive, dashed contours negative.